STATISTICA, anno LXXXIII, n. 1, 2023

JOINT MONITORING USING INFORMATION THEORETIC CONTROL CHARTS

Moiz Quershi
Government Degree College Tandojam, District Hyderabad, Sindh
Department of Statistics, Quaid-i-Azam University, 45320, Islamabad, Pakistan

Sajid Ali[1]
Department of Statistics, Quaid-i-Azam University, 45320, Islamabad, Pakistan

Ismail Shah
Department of Statistical Sciences, University of Padua, 35121, Padova, Italy
Department of Statistics, Quaid-i-Azam University, 45320, Islamabad, Pakistan

SUMMARY

Statistical process control consists of sophisticated and well-organized methods which contribute to monitor and improve the quality of a product. Control charts are now routinely used in many applied areas to enhance the quality of products. In this study, a general framework is presented to construct univariate control charts for joint monitoring using the information theoretic approach. To this end, we monitor a process by maximizing the entropy and by minimizing the cross entropy. Information control charts are free from strict distributional assumptions, as information charts are based on information discrepancy between the initial moment μ_0 and the data moments r_t. These charts can jointly monitor mean and variance and thus provide a unified approach that is helpful in reducing the labor for designing separate charts. Besides real data applications, in this study, Monte Carlo simulations are used to assess the performance of the information charts using the average run length as a performance criterion assuming different distributions including normal, gamma, exponential, lognormal, Weibull and beta. Furthermore, a comparison with the traditional charts is also given for each distribution.

Keywords: Shewhart chart; Information theoretic charts; Kullback-Leibler; Weibull distribution; Lognormal distribution

1. INTRODUCTION

The historical background of quality is as ancient as the industry. The basic purpose to use the quality control is to get rid of the system failure and consumers claims by pro-

[1] Corresponding Author. E-mail: sajidali.qau@hotmail.com

viding a quality product. Consequently, improving the quality of a product or service is the main factor that links to the success of a business. Statistical process control (SPC) is defined as the set of statistical tools that are used to monitor, control and hence, improve the quality of the output of a production system. Among the SPC tools, control charts are successfully used to monitor the quality of a process. A process is said to be statistically in-control if it is monitored only in the presence of natural cause, which can never be eliminated from the process. However, a process is said to be statistically out-of-control when it is being monitored in the presence of external causes that are also called as the special cause variation. The basic aim of a control chart is to detect the assignable (external) cause as early as possible.

This article focuses on the information theoretic framework for process monitoring using the maximum entropy (ME) function and minimum discrimination information (MDI) function. More specifically, the aim of this study is to assess monitoring strategies for different distributions using information theoretic methods for joint moments monitoring of the process by a single control chart. The performance of the proposed charts is evaluated using the average run length (ARL) criterion. Further, a comparison of the information theoretic control charts with the traditional memory-less control charts is also discussed in this study.

Many researchers focused on the mean monitoring (Ahmed *et al.*, 2022; Raza *et al.*, 2021; Ali *et al.*, 2021; Raza and Siddiqi, 2017; Aslam *et al.*, 2018; Ali, 2017; Nabeel *et al.*, 2021), however, the joint monitoring of mean and variance is also a very popular topic, see for example Saniga (1977), White and Schroeder (1987), Chen and Cheng (1998), Celano *et al.* (2016), Ramadan (2018), Domangue and Patch (1991), Gan (1995), Chen *et al.* (2001), Chen *et al.* (2004), Khoo *et al.* (2010), Mukherjee and Chakraborti (2012), Mukherjee *et al.* (2015), Li *et al.* (2016) and references cited therein for monitoring mean and variability (or location and spread). The use of information theory in statistical problems is very common, see for example Jaynes (1957), Brockett (1991), Soofi *et al.* (1995), Sawa (1978), and references cited therein.

Alwan *et al.* (1998) introduced a general theory for constructing control charts based on the information theory to monitor the moments of a distribution using a single charting scheme. The proposed approach is based on the process moments which are mapped to an in-control distribution moments and then the Kullback-Leibler (cross entropy) is used with some constraints to mark the discrepancy between the in-control and monitoring moments. Thus, the information charts are made without using any specific distributional assumptions. The authors developed an information mean variance (IMV) chart based on the normal distribution. By comparing IMV chart with the standard chart using the average run length (ARL), it was shown that the IMV chart performs better than the $\bar{x}$ and s^2 charts. Recently, Chang and Chen (2020) proposed a Kullback-Leibler based control chart for monitoring linear profile for phase-II analysis. The authors also made a comparison between the proposed and existing generalized likelihood ratio (GLR) charts and numerically they showed that the proposed chart outperforms the existing chart.

Chen *et al.* (2001) proposed a new exponentially weighted moving average (EWMA) chart to detect decrease and increase mean shifts in the process. Khoo *et al.* (2010) proposed a maximum double EWMA chart by constructing the charting statistic using the maximum of absolute values of two DEWMA statistics to control the mean and variance. The authors concluded that the proposed chart outperformed for detecting moderate and small changes in mean or variance of a process than the Max-EWMA chart. Chen *et al.* (2004) designed an EWMA-SC chart to efficiently monitor simultaneously the mean and variation of a normal process. It is concluded that this chart is efficient in detecting the source and the direction of out-of-control signal with the desirable properties. Mukherjee *et al.* (2015) proposed a control chart for monitoring the simultaneous location and variation using a single chart assuming two-parameter exponential distribution. The monitoring statistic of the proposed chart is based on the maximum likelihood estimator and it is concluded that the propose chart performs better when the sample size is large. Li *et al.* (2016) proposed two maximum cumulative sums (CUSUM) charts which naturally work better in the situation when the process parameters are unknown. Using a numerical study, it is shown that the proposed charts outperform in detecting small to moderate shifts in location and scale than the Shewhart type control chart. Chang and Chen (2020) proposed a Kullback-Leibler based control chart for monitoring linear profile for phase-II analysis. The authors also made a comparison between the proposed and existing generalized likelihood ratio (GLR) chart and it is shown that the proposed chart outperforms the existing chart. The average time to signal (ATS) is used to assess the performance of the proposed control chart. Chatterjee *et al.* (2023) proposed a parametric generally weighted moving average (GWMA) maximum control chart for simultaneous monitoring the location and scale parameters. The author also compared this chart with EWMA-Max and DEWMA-Max using the ARL criterion and from the results it is noticed that GWMA-Max chart detects the small shift in simultaneously process efficiently. We refer to Takemoto and Arizono (2023) for recent directions related to information theoretic charts.

Mukherjee and Chakraborti (2012) proposed a single nonparametric Shewhart-type control chart for joint monitoring the location and dispersion of the process in situation when the both parameters are unknown. The charting statistic is based on the Wilcoxon sum rank test that monitors the mean and dispersion by using the Ansari–Bradley statistic. The effect of reference observations is also investigated and it is found that the reference sample size 100 or 150 is required to get the in-control ARL in the phase-I analysis. Celano *et al.* (2016) conducted a study on the comparison of different control charts which monitor the location and scale for observations having a location-scale distribution in a finite horizon process. The authors applied distribution-free singed rank statistics to monitor the location and robust estimators to monitor the scale of the process. Results showed that the singed rank statistics outperformed for monitoring the location and Downton's D estimator outperformed in monitoring the scale of the process for non-normal data when the observations follow the uniform distribution. In addition, if the data follow the normal distribution, Downton's D estimator provides the best result to monitor the scale of the process. Chakraborti and Graham (2019) discussed nonparametric charts. Chowdhury *et al.* (2015) proposed a distribution free nonparametric

CUSUM Shewhart chart based on Lepage statistic for simultaneous monitoring. This chart is compared with Shewhart chart and found that the CLS chart outperform than existing chart for location and scale. Also, Chowdhury *et al.* (2014) proposed a nonparametric control chart for joint monitoring the mean and variance of the process. This proposed chart is based on the Cucconi statistic and named as the Shewhart-Cucconi (SC) chart. Authors also compared proposed chart with Shewhart-Lepage chart and found that the proposed chart is efficient in monitoring the joint process efficiently. Chang and Wu (2022) also proposed exponential time-between-event chart by estimating the rate parameter using the maximum likelihood estimator, the uniformly minimum variance unbiased estimator, and the minimum mean squared error estimator.

Boone and Chakraborti (2012) considered two multivariate distribution-free control charts. Das and Bhattacharya (2008) proposed a nonparametric control chart to monitor scale the variability of a process. To check the efficiency of the proposed chart, the authors compared it with the S-type Shewhart control chart and found that the proposed chart outperformed than S-chart. Das (2009) proposed a multivariate nonparametric control chart based on bivaraite sign test. The author also made a comparative analysis between proposed and multivariate normal and t distribution charts. Ghadage and Ghute (2023) proposed a nonparametric control chart to monitor the location and scale parameters of the process. The proposed chart is compared with nonparametric Shewhart-Cucconi (SC) and Shewhart-Lepage (SL) charts and found that the proposed chart outperformed than the existing comparative chart. More recently, Xue *et al.* (2023) proposed a novel nonparametric EWMA control chart to monitor count and continuous data. The proposed chart is compared with the existing charts and found that the proposed chart efficiently handle the situation of false alarm in monitoring the process.

McCracken and Chakraborti (2013) presented an overview study based on one and two control chart scheme for the case of known and unknown parameters. This study also discussed the joint monitoring scheme for the multivariate, auto-correlated and individual process. Ramadan (2018) discussed a simple model for economic statistical design of joint $\bar{x}$-chart and s^2-chart. Fuzzy multi-objective modeling constraints were used to obtain the weighted average for measuring the satisfaction level. A comparative analysis between joint $\bar{x}$,s^2 and $\bar{x}$, s chart is presented to enhance the effectiveness in detecting the special cause variations.

In this article, we consider the known standards for the information theoretic framework, which is similar to Alwan *et al.* (1998), and using these in-control parameters we study the in-control and out-of-control situations by using the Kullback-Leibler. Also, we construct the joint control charts based on information theoretic framework and compared them with Shewhart-type individual mean and variance control chart. To this end, two-sided control limits are used and based on the ARL criterion, the decisions are made.

The rest of the article is organized as follows. Section 2 introduces the main framework for the information theoretic control charts. The performance of different information theoretic control charts assuming exponential, gamma, Weibull, normal, lognormal, and beta distribution is discussed in Section 3. Concluding remarks are given in Section 4.

2. Information Theoretic Control Charts

In this Section, the maximum entropy (ME) (Jaynes, 1957; Shore and Johnson, 1980) and the minimum discrimination information (MDI) Kullback (1959) statistics are used to design the information theoretic process control (ITPC) charts to monitor the process moments. To this end, we assume that the actual data generating process is unknown (Sawa, 1978) and some sort of averages are used to approximate the data generating distribution. The constrained functional optimization method utilizes the pre-specified and true moments of the data to estimate $f_0^*(z|\mu_0, \sigma_0^2)$ of the process distribution and $f_t^*(z|\bar{z}_t, s_t^2)$ for the in-control state at each monitoring time t. Then, an information control function $D_{\mathrm{KL}}(f_0^*, f_t^*)$ measures the difference between monitoring state and in-control state. Let us monitor a number of process moments by

$$S_\lambda = E_f[g_\lambda(Z)] = \int g_\lambda(z)\mathrm{d}F(z), \qquad \lambda_i = 0, 1, 2, \ldots, \lambda_m \tag{1}$$

where $g_0(z) = 1$ and λ_i are the numbers of Lagrange multipliers to enforce the constraints that normalize the density, f and g_{λ_i} are absolutely integrable functions with respect to dF. Further, let $\mu_0 = (\mu_{10}, \mu_{20}, \ldots, \mu_{\lambda_{\mathrm{m}0}})$ represent the in-control moments of the process based on the engineering design or assuming known parameters. The in-control moments μ_0 and data moments $\mathbf{r_t} = (\mathbf{r_{1t}}, \mathbf{r_{2t}}, \ldots, \mathbf{r}_{\lambda_{\mathrm{mt}}})$ computed from the samples $\mathbf{z_t} = (\mathbf{z_{t1}}, \mathbf{z_{t2}}, \ldots, \mathbf{z_{tn}})$ at time t are the only information available to monitor the process $f(z|\mu)$.

The conventional control charts assume that the process follows a specific distribution which may not be a true assumption in practice. The ITPC method consists of three operational steps to monitor the moments. First, use the ME principle which takes the in-control moments $\mu_{\lambda_{m0}}$ as the input and results in a model $f_0^*(z|\mu_0)$ to obtain an estimated model of the unknown process distribution $f(z|\mu)$ for the in-control state. Then, the distribution of the process is estimated at each monitoring state. At the third step, MDI statistic is used to detect the changes occurred in the monitoring distribution as well as in-control state.

Entropy is defined as an average amount of uncertainty that a random variable possess or, equivalently, it is defined to represent the degree of randomness. Mathematically, the entropy of a probability distribution can be expressed as

$$H(Z) \equiv H[f(z)] = -\int \log f(z)\mathrm{d}F(z). \tag{2}$$

A general model is formulated on the basis of ME principle at the in-control state for process monitoring (Rajan *et al.*, 2018)

$$S_0 = \{f(z|\mu_0) : \int g_\lambda(z)\mathrm{d}F(z|\mu_0) = \mu_{\lambda_{m0}},\ \lambda_i = 0, 1, 2, \ldots, \lambda_m\}. \tag{3}$$

In statistics, many distributions fulfill the moment constraints. The ME model $f_0^*(z|\mu_0)$ is obtained by maximizing $H(z|\mu_0)$ with respect to the density f over S_0 for a stable or in-control state. Using the variational calculus with Lagrangian multiplier

$$\mathscr{L} = -\int \log f(z|\mu_0) - \sum_{\lambda_i=0}^{\lambda_m} \eta_{\lambda_i} \int [\mathbf{g}_\lambda(\mathbf{z}) - \mu_{\lambda_0}] \mathrm{d}\mathbf{F}(\mathbf{z}|\mu_0), \tag{4}$$

the result is obtained by taking the derivative of $\mathscr{L}$ with respect to density f. The first order condition of Lagrangian $\mathscr{L}$ may not give the specified moments for an in-control process but if exits it can be obtained in the form

$$f_0^*(z|\mu_0) = \mathbf{C}(\mu_0) \exp\left\{ \sum_{\lambda_i=1}^{\lambda_m} \eta_{\lambda_i}(\mu_0) g_\lambda(z) \right\}, \tag{5}$$

where $\mathbf{C}(\mu_0)$ represents the normalizing constant for the density and $\eta_{\lambda_i}(\mu_0)$, $\lambda_i = 1, \ldots, \lambda_m$ are the Lagrange multiplier to enforce the constraints of Eq. (3) (Kapur, 1989). The symbol f_0^* denotes the estimated ME model of true distribution f to monitor the moments of the process. The ME model $f_0^*(z|\mu_0)$ is just an information theoretic (IT) estimate of $f(z|\mu)$ which utilizes moments constraint in Eq. (3) to estimate the unknown true probability distribution $f(z|\mu)$. Using suitable $g_\lambda(z)$, most of the parametric distributions can be written by the ME result, for example, Table 1 lists many MEs for different distributions.

TABLE 1
Maximum Entropy Distributions.

Parameter(s) of interest $\mu_{\lambda_m} = E_f[g_\lambda(Z)]$	ME distribution
$\mu_1 = E(Z)$, $\mu_2 = E(Z-\mu_1)^2$	Normal
$\mu_1 = E\|Z\|$, $\mu_2 = E\|Z-\mu_1\|$	Laplace
$\mu_\lambda = E(Z^{\lambda_m})$, $\lambda_i = 1, 2, \ldots, \lambda_m$	K-Exponential
$\mu_1 = E(Z)$, $z > 0$	Exponential
$\mu_1 = E(Z)$, $\mu_2 = E(\log Z), z > 0$	Gamma
$\mu_1 = E(Z^a)$ $a \neq 1$, $\mu_2 = E(\log Z), z > 0$	Weibull
$\mu_1 = E(Z)$, $\mu_2 = E[(\log Z)^2], z > 0$	Log-Normal
$\mu_1 = E(Z)$, $\mu_2 = E[\log(1-Z)], 0 < z < 1$	Beta

2.1. Formulation of Monitoring Distribution

Two types of information are required to approximate the process distribution at the monitoring point. The first one is the in-control process distribution $f_0^*(z|\mu_0)$ and the second one is the vector of data moments $\mathbf{r_t}$. In particular, we take into account the distribution class

$$S_t = \left\{ f(z|\mathbf{r_t}) : \int g_\lambda(z) \mathrm{d}F(z|r_t) = r_{\lambda_t}, \lambda_i = 0, 1, \ldots, \lambda_m \right\}, \tag{6}$$

which is nearest to the in-control ME distribution $f_0^*(z|\mu_0)$ suitable to monitor the process. The Kullback-Libeler discrimination information statistic D_{KL} is used to calculate the difference between reference distribution F_0^* and monitoring process F_t.

$$D_{\mathrm{KL}}(f_t : f_0^*) = \int \log\left(\frac{f_t}{f_0^*}\right) \mathrm{d}F_t(z) \geq 0. \tag{7}$$

The equality holds if $F_t = F_0^*$ approximately. The function D_{KL} is also called the cross or relative entropy. The ITPC links the current information and the in-control distribution using the MDI theory. The MDI leads to probability which minimizes $D_{kL}(f_t : f_0^*)$ in relation to f_t over S_t. Thus, the MDI provides a general structure of the solution (Kullback, 1959). Also, it would lead to a similar family as f_0^* where parameters are obtained by moments of data r_t. In this case, the reference distribution $f_0^*(z|\mu_0)$ is the ME model, one can derive the MDI solution in a simple form. To demonstrate it, we expand $D_{kL}(f_t : f_0^*)$ by using Equations from 3 to 6 as follows

$$\begin{aligned} D_{\mathrm{KL}}(f_t : f_0{}^*) &= \int \log f_t(z|\mathbf{r_t}) \mathrm{d}F(z|\mathbf{r_t}) - \int \log f_0{}^*(z|\mu_0) \mathrm{d}F(z|\mathbf{r_t}) \\ &= -H[f_t(z|\mathbf{r_t})] - \mathbf{E_t}[\log \mathbf{f_0}{}^*(\mathbf{z}|\mu_0)] \\ &= -H[f_t(z|\mathbf{r_t})] - \log \mathbf{C}(\mu_0) - \sum_{\lambda_\mathrm{i}=1}^{\lambda_\mathrm{m}} \eta_{\lambda_\mathrm{i}}(\mu_0) \mathbf{E_t}[\mathbf{g}_\lambda(\mathbf{Z})] \\ &= -H[f_t(z|\mathbf{r_t})] - \log \mathbf{C}(\mu_0) - \sum_{\lambda_\mathrm{i}=1}^{\lambda_\mathrm{m}} \eta_{\lambda_\mathrm{i}}(\mu_0) \mathbf{r_t} \end{aligned} \tag{8}$$

and the resulting MDI solution is

$$f_t^*(z|\mathbf{r_t}) = C(\mathbf{r_t}) \exp\left\{ \sum_{\lambda_i=1}^{\lambda_m} \eta_{\lambda_i}(\mathbf{r_t}) g_\lambda(z) \right\}. \tag{9}$$

Using the reference distribution f_0^* and the moment constraints as given in Eq. (1), one can obtain $f_t^*(z|r_t)$ which is the information theoretic estimate of the true unknown distribution $f(z|\mu)$ for the process monitoring variable.

2.2. Information Control Function

The model in Eq. (9) is an approximate form of the constraint given in Eq. (5). Now, to monitor the process at time t, the MDI function is used to measure the information difference between the monitoring state $f_t^*(z|\mathbf{r_t})$ and the in-control state $f_0^*(Z|\mu_0)$. If the difference between monitoring state and in-control state is large, the process is considered as out-of-control. Thus, by determining the ME value we achieve the MDI control function that can monitor shifts in the parameter values.

$$H[f_t^*(z|\mathbf{r_t})] = -\log C(\mathbf{r_t}) - \left\{ \sum_{\lambda_i=1}^{\lambda_m} \eta_{\lambda_i}(\mathbf{r_t})\mathbf{r}_{\lambda_t} \right\} \tag{10}$$

Substituting Eq. (10) in Eq. (8), the MDI control function can be written as

$$\begin{aligned} I_{r_t} &= 2nD_{\mathrm{KL}}(f_t : f_0^*) = 2n\{-H[f_t^*(z|\mathbf{r_t})] - E_t[\log f_0^*(Z|\mu_0)]\} \\ &= 2n\left\{ \log \frac{\mathrm{C}(\mathbf{r_t})}{\mathrm{C}(\mu_0)} + \sum_{\lambda_i=1}^{\lambda_m} [\eta_{\lambda_i}(\mathbf{r_t}) - \eta_{\lambda_i}(\mu_0)]\mathbf{r}_{\lambda_t} \right\}. \end{aligned} \tag{11}$$

The function I_{r_t} is the smallest information difference of variation between $f_0^*(z|\mu_0)$ and $f_t^*(z|\mathbf{r_t})$ for process monitoring variable $f(z|\mu)$. Further, I_{r_t} is also referred to as the function of the in-control moments and monitoring moments value of a process. By I_{r_t} function, we analyze and compare the process monitoring to the in-control state in a sequential order. If there is a difference between the moment values then the MDI between $f_0^*(z|\mu_0)$ and $f_t^*(z|\mathbf{r_t})$ would also be different for a process monitoring variable $f(z|\mu)$. If this information difference is sufficiently large and outside the control limits, the process will be considered as the out-of-control.

To formulate the information control function, moment values be used to obtain the Lagrangian multipliers $\eta_{\lambda_i}(\mathbf{r_t})$ and $\eta_{\lambda_i}(\mu_0)$. Then, using Eq. (11) the information control function I_{r_t} is calculated. Some MDI functions $D_{\mathrm{KL}}(f_t : f_0^*)$ for different well-known ME model distributions are shown in Table A.1 in the Appendix. We present the performance evaluation of information theoretic control charts in the next Section using these MDI functions.

3. Performance of the Information Theoretic Control Charts

To study the performance of the MDI function based charts for different distributions using Monte Carlo simulations as well as real data sets, we assess the performance by using the zero-state ARL, which is a commonly used criterion. The ARL is defined as the average number of points taken before detecting an out-of-control signal. More specifically, when the subgroup size is larger than 1 ($n > 1$), the ARL is the average number of subgroups (samples) taken before an out-of-control signal shows up on a control chart. It is to be noted that Jalilibal *et al.* (2022) pointed out that the control chart performance evaluated on the basis of zero-state ARL is fundamentally flawed. However, in our opinion, the importance of zero-state ARL cannot be ignored as zero-state and steady-state performances serve different perspectives. In particular, zero-state performance is particularly more important for noting a shift at the beginning or within the first few samples.

3.1. IMV_t Chart for Normal Distribution

Normal distribution is one of the most widely distributions in statistics and statistical quality control. To develop the normal distribution control chart, we required two parameters, mean μ and variance σ^2. For the information control chart, it is assumed that the in-control parameters, i.e., (μ_0, σ_0^2) are known. Using the formulation of Section 2, the population moments are defined as

$$\mu_{10} = \int z f_0(z) \mathrm{d}z \tag{12}$$

$$\mu_{20} = \int (z - \mu_{10})^2 f_0(z) \mathrm{d}z \tag{13}$$

and S_0 is determined by these two moments in Eq. (12) and Eq. (13). From Table 1, it is observed that the ME result over the distribution in S_0 is $f_0^*(z|\mu_0, \sigma_0^2)$ that is a normal with mean μ_0 and variance σ_0^2 where the model parameters are obtained by the moment equations given in Table A.1. Let the sample mean and variance are denoted by r_{1t} and r_{2t}, respectively. To express the class of S_t distributions, we replace μ_{10} and μ_{20} in Eq. (12) and Eq. (13) by data moments r_1t and r_2t and then the MDI distribution in S_t with relation to $f_0^*(z|\mu_0, \sigma_0^2) = N(\mu_0, \sigma_0^2)$ is estimated. Then the MDI equation becomes $f_t^*(z|\bar{z}_t, z_t^2) = N(\bar{z}_t, z_t^2)$ which is considered as the approximate distribution for the in-control process that satisfies the moment constraints. Using the results of Table A.1, the MDI control function for the normal distribution can be written as

$$\begin{aligned} 2nD_{KL_t}(f_t{}^* : f_0{}^*|\mu_0, \sigma^2, \bar{z}_t, z_t^2) &= 2n\left[\frac{(\bar{z}_t - \mu_0)^2}{2\sigma_0^2} + \frac{1}{2}\left[\frac{z_t^2}{\sigma_0^2} - \log\frac{z_t^2}{\sigma_0^2} - 1\right]\right] \\ &= \frac{n(\bar{z}_t - \mu_0)^2}{\sigma_0^2} + n\left[\frac{z_t^2}{\sigma_0^2} - \log\frac{z_t{}^2}{\sigma_0^2} - 1\right]. \end{aligned} \tag{14}$$

The first term in Eq. (14) evaluates the information discrepancy as a result of process mean while the second term evaluates the process variability. This equation can be written as $\mathrm{IMV}_t = \mathrm{IM}_t + \mathrm{IV}_t$, where

$$\mathrm{IM}_t = 2nD_{KL_t}(f_t^* : f_0^* | \mu_0, \bar{z}_t, \sigma^2) = \frac{n(\bar{z}_t - \mu_0)^2}{\sigma_0^2} \tag{15}$$

$$IV_t = 2nD_{KL_t}(f_t^* : f_0^* | \sigma^2, z_t^2, \mu_0) = n\left[\frac{{z_t}^2}{\sigma_0^2} - \log\frac{{z_t}^2}{\sigma_0^2} - 1\right]. \tag{16}$$

Thus, IM_t can be used to diagnose mean shift and IV_t for the variance shift. By adding and subtracting $\frac{z_t^2}{\sigma_0^2}$ in Eq. (16), it can be written as

$$\frac{(n-1)z_t^2}{\sigma_0^2} + \left[\frac{z_t^2}{\sigma_0^2} - n\log\frac{z_t^2}{\sigma_0^2} - n\right]. \tag{17}$$

Now using Eq. (17), the upper percentiles using $\mu_0 = 0$, $\sigma_0^2 = 1$ and $\alpha = 0.0027$ for different $n = 3, \ldots, 15$ are listed in Table 2 by using 100000 Monte Carlo simulation runs. Here, it is to be noted that the lower percentiles are zero for the IMV chart. It is clear from the table that the UCL decreased as the sample size increased.

TABLE 2
Upper Percentile of Information Mean variance IMV_t Chart for Normal Distribution assuming $\alpha = 0.0027$.

n	3	4	5	6	7	8	9	10	11	12	13	14	15
UCL	16.03	14.98	13.90	13.40	13.10	12.98	12.73	12.40	12.05	11.95	11.80	11.68	11.62

3.1.1. Average Run Length for Normal Distribution

This Section presents the ARL study by using the Monte Carlo simulations to test the effectiveness of the IMV_t chart for the normal process. Using different sample sizes for $N(0,1)$ process, the ARL values with standard deviation of run length (SDRL) are reported in Table 3. It is noticed from the table that ARL_0 varies from sample to sample and the nominal value (370) is achieved at $n = 4$. To study the out-of-control performance, we introduced mean and variance shifts in the in-control process. To this end, the in-control mean shifted from μ_0 to out-of-control mean μ_1 while the in-control variance σ_0^2 to σ_1^2. Thus, the mean shift is denoted by $\delta = \frac{\mu_0 - \mu_1}{\sigma_0}$ and variance shift is denoted by $k = \frac{\sigma_1}{\sigma_0}$. Further, we suppose that δ and k ranges from 0 to 2 with the increment of 0.2. It is notable that we only consider upward shifts because these are the most important and must be detected as soon as possible. Table 4 lists the out-of-control ARL for n=4 based on 100000 Monte Carlo simulations. It can be observed from the table that the IMV_t chart performs better when there is a mean shift for fixed variance shift. Similarly, a dispersion shift is detected more quickly for the fixed mean shift and for fixed variance, a pure mean shift will take more points to detect it and vice versa.

TABLE 3
ARL and SDRL for information mean variance chart for Normal Distribution at α=0.0027.

α	n	3	4	5	6	7	8	9	10	11	12	13	14	15
0.0027	ARL	283.40	372.50	337.30	355.20	328.30	360.80	323.35	315.30	278.54	261.60	240.80	239.60	229.08
	SDRL	283.30	372.50	339.47	355.43	346.00	351.40	322.45	327.05	258.74	257.16	229.10	236.00	233.25

3.1.2. Real Data Application

To show a practical application of the normal IMV_t chart, a data set about the number of defects in painted automobile hoods is taken from Montgomery (2019). For comparisons, we apply the $\bar{X}$, S^2 and IMV_t charts, where the control limits for standard $\bar{X}$ chart are given below in Eq. (18) and Eq. (19) and the control limits for variance chart are given in Eq. (20) and Eq. (21).

$$\mathrm{LCL} = \hat{\mu} - z_{\frac{\alpha}{2}} * \hat{\sigma}, \tag{18}$$

$$\mathrm{UCL} = \hat{\mu} + z_{\frac{\alpha}{2}} * \hat{\sigma}, \tag{19}$$

$$\mathrm{LCL} = \frac{\bar{S}^2}{n-1} * \chi^2_{\frac{\alpha}{2}, n-1}, \tag{20}$$

$$\mathrm{UCL} = \frac{\bar{S}^2}{n-1} * \chi^2_{1-\frac{\alpha}{2}, n-1}. \tag{21}$$

It can be noticed from frame (a) of Figure 1 that the LCL(=1.44) of the $\bar{X}$ chart does not detect out-of-control signal. On the other hand, the S^2 chart depicted in frame (b) of Figure 1 signals out-of-control at the twenty-eight sample. Compared to these both charts, IMV_t chart depicted in frame (c) of Figure 1 signals out-of-control at the thirty-second sample with the UCL. However, the IMV chart get first out-of-control signal at 6th point by using the LCL(=30.68). Hence, the IMV_t chart outperforms the existing control charts.

3.2. IMV_t Chart for Gamma Distribution

Gamma distribution is a positively skewed and extensively used in statistics and quality control. For example, Torng *et al.* (2009) utilized Tukey control chart to monitor the gamma distribution for short-run process. Derya and Canan (2012) used weighted variance, weighted standard deviation, and skewness correction methods based control

TABLE 4

ARL and SDRL for information mean variance chart for Normal Distribution at $\alpha = 0.0027$ for $n = 4$.

k	0.2		0.4		0.6		0.8		1.0		1.2		1.4		1.6		1.8		2	
δ	ARL	SDRL	ARL	SDRL	ARL	SDRL	ARL	SDRL	ARL	SDRL	ARL	SDRL	ARL	SDRL	ARL	SDRL	ARL	SDRL	ARL	SDRL
0.0	8.52	8.03	55.50	54.55	164.98	163.40	329.10	328.45	372.50	372.50	102.00	102.00	25.75	25.40	10.00	9.70	5.25	4.90	3.47	3.20
0.2	8.00	7.45	52.65	51.70	154.40	154.80	294.35	294.35	300.00	299.00	83.50	82.20	22.85	22.25	9.20	8.70	5.10	4.50	3.4	2.9
0.4	6.80	6.26	42.73	41.59	118.32	118.70	208.25	210.40	170.0	169.20	53.40	53.20	17.80	17.20	7.90	7.40	4.70	4.10	3.20	2.70
0.6	5.30	4.77	30.70	29.75	80.20	80.03	120.60	121.50	81.00	80.00	30.45	30.20	12.53	11.90	6.60	5.90	4.10	3.50	3.05	2.45
0.8	3.76	3.18	20.25	20.02	46.32	45.43	57.40	57.50	36.05	35.20	17.25	16.40	8.80	8.40	5.20	4.60	3.50	3.10	2.80	2.40
1.0	2.5	1.95	11.40	10.90	23.65	23.06	25.90	25.10	17.50	16.90	10.05	9.40	6.10	5.40	4.10	3.70	3.10	2.50	2.40	1.90
1.2	1.70	1.10	6.05	5.50	11.15	10.70	11.60	11.20	8.80	8.10	6.10	5.80	4.30	3.75	3.20	2.80	2.60	2.10	2.20	1.50
1.4	1.25	0.65	3.20	2.65	5.40	4.90	5.75	5.20	5.00	4.35	4.00	3.50	3.15	2.60	2.60	2.00	2.20	1.60	2.00	1.30
1.6	1.05	0.60	1.85	1.25	2.80	2.30	3.20	2.65	3.10	2.50	2.70	2.15	2.40	1.80	2.10	1.50	1.90	1.30	1.70	1.10
1.8	1.00	0	1.30	0.70	1.80	1.20	2.10	1.50	2.15	1.50	2.05	1.50	1.90	1.30	1.80	1.20	1.65	1.00	1.60	1.00
2.0	1.00	0	1.05	0.30	1.30	0.70	1.50	0.90	1.60	1.00	1.60	1.00	1.50	1.00	1.40	0.90	1.40	0.85	1.35	0.80

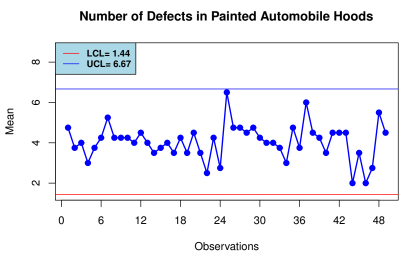

(a) $\bar{X}$ Chart

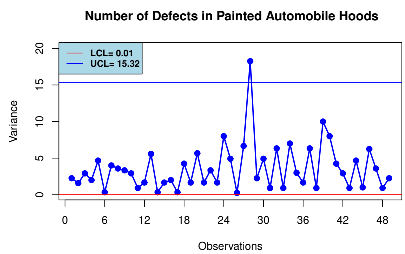

(b) S^2 Chart

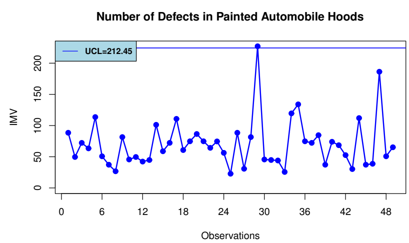

(c) IMV_t Chart

Figure 1 – Comparison of $\bar{X}$, S^2 and IMV_t Charts for the Number of Defects in Painted Automobile Hoods.

charts assuming gamma, Weibull, and log-normal distributions. Hao *et al.* (2016) proposed gamma control chart with known parameter case and concluded that this chart is efficient in detecting shifts in the scale parameter. Aslam *et al.* (2017) proposed a control chart based on multiple dependent state sampling for gamma distributed quality characteristics. We obtain the upper and lower percentiles of the gamma distribution based chart using Monte Carlo simulations with the following MDI function.

$$
\begin{aligned}
2nD_{KL_t}(f_t^* : f_0^* | \mu_{10}, \mu_{20}, r_{1t}, r_{2t}) = 2n\Big[-\log \frac{(\theta_t)^{k_t}\Gamma(k_t)}{(\theta_0)^{k_0}\Gamma(k_0)} + \frac{r_{1t}}{\mu_{10}} k_0 - \\
k_t + (k_t - k_0) r_{2t} \Big]. \qquad (22)
\end{aligned}
$$

This distribution has two unknown parameters, i.e., k_t and θ_t, and we estimate them using the maximum likelihood method. In particular, Nelder-Mead iterative search (Holland and Fitz-Simons, 1982; Delignette-Muller *et al.*, 2015) using R language is used. To study the performance, we set in-control parameters $k_0 = 1, \theta_0 = 1$ using $\alpha = 0.0027$ and α=0.0047, respectively, and find the upper and lower percentiles (or LCL and UCL) for $n = 3, \ldots, 15$ using Monte Carlo simulations. The results of upper and lower percentiles based on 100000 replications are listed in Table 5. It can be noticed from Table 5 that as sample size increases, the LCL and UCL of gamma distribution decrease. For calculating the out-of-control ARL, we introduced artificial shifts in the parameters, i.e., k_0 and θ_0, $n = 6, 7$ with fixed $\mathrm{ARL}_0 = 200$ to evaluate the performance of IMV_t gamma control chart. Table 6 assesses the effect of different sample sizes on the in-control ARL. It is clear that $n = 7$ yields the $\mathrm{ARL}_0 = 212$. Next, we introduce different size shifts and study the out-of-control performance of the IMV_t control chart. The results listed in Table 6 indicate that the chart is efficient for downward shifts in the scale parameter while it takes more points to detect out-of-control signals if k is large. It is also noticed that the large shifts are detected more quickly than small shifts.

TABLE 5
Lower and Upper percentiles of IMV_t Chart for Gamma Distribution.

	$\alpha = 0.0027$		$\alpha = 0.0047$	
n	LCL	UCL	LCL	UCL
3	24.05	152.14	29.10	200.40
4	14.31	52.12	14.08	56.63
5	11.03	36.94	11.00	29.48
6	7.26	33.50	9.23	28.56
7	7.24	19.57	7.20	27.50
8	7.23	15.52	7.15	15.17
9	7.10	14.40	7.10	14.30
10	6.90	13.60	6.96	13.39
11	6.85	12.80	6.85	12.92
12	6.72	12.74	6.32	12.71
13	6.43	12.57	6.15	12.60
14	6.35	12.50	6.07	12.55
15	6.23	11.86	6.00	12.52

TABLE 6
ARL and SDRL for IMV_t chart for gamma distribution.

n		3	4	5	6	7	8	9	10	11	12	13	14	15
6	ARL	85.74	61.52	79.36	210.00	130.55	77.09	77.36	62.97	62.63	127.06	83.15	114.29	54.96
	SDRL	70.14	58.84	68.45	93.75	81.66	61.08	67.85	56.52	59.30	86.12	70.72	83.07	53.37
7	ARL	92.18	84.76	66.30	118.35	212.40	95.70	53.70	67.05	48.65	92.15	91.40	113.30	107.20
	SDRL	74.80	72.80	55.10	81.80	56.50	77.75	49.50	58.00	47.60	72.90	74.81	79.32	82.40

Next, Table 7 and Table 8 list the out-of-control ARL for fixed scale parameter while shifting the shape parameter of the gamma distribution. Table 9 lists ARL_1 results assuming simultaneous shifts in the both parameters of the gamma distribution and it is clear that upward shifts are detected more quickly than the downward shifts.

TABLE 7

ARL and SDRL assuming k_0 fixed while θ_0 varies.

n	δ	0.60	0.65	0.70	0.75	0.80	0.85	0.90	0.95	1.05	1.10	1.15	1.20	1.25
6	ARL	1.0	1.10	1.36	4.52	21.05	88.90	133.42	134.85	162.35	21.30	8.30	4.02	1.20
	SDRL	0.0	0.10	1.18	4.15	21.47	74.36	86.41	84.73	108.30	42.70	2.26	0.63	0.0
7	ARL	1.0	1.07	1.10	1.85	11.50	94.20	141.90	154.95	162.35	21.30	8.30	4.02	1.20
	SDRL	0.0	0.10	0.90	1.25	9.35	75.60	92.60	85.90	70.55	20.22	8.17	3.98	0.80

TABLE 8

ARL and SDRL when θ_0 parameter is fixed and k_0 varies.

δ	0.60	0.65	0.70	0.75	0.80	0.85	0.90	0.95	1.05	1.10	1.15	1.20	1.25	1.30	1.35	1.40
ARL	1.0	1.04	1.20	2.10	6.24	41.31	103.52	146.18	146.33	125.5.0	19.5.0	3.33	1.36	1.06	1.01	1.0
SDRL	0	0.20	0.50	1.50	5.87	38.20	45.96	78.72	89.10	85.51	20.08	2.52	0.76	0.23	0.10	0

TABLE 9
ARL and SDRL when θ_0 parameter is fixed while k_0 varies.

δ	0.75	0.80	0.85	0.90	0.95	1.05	1.10	1.15	1.20	1.25	1.30	1.35	1.40	1.45	1.50	1.55	1.60	1.65	1.70	1.75	1.80	1.85	1.90	1.95	2.0
ARL	1.20	4.10	10.10	77.21	170.40	142.20	140.33	139.20	136.05	135.05	126.50	102.10	75.37	41.90	23.90	13.90	8.75	5.45	3.65	2.90	2.10	1.70	1.40	1.20	1.0
SDRL	0.70	3.10	9.80	83.92	91.33	94.50	97.23	88.75	84.65	85.80	84.20	74.40	66.90	42.60	22.55	13.70	8.10	4.75	3.00	2.55	1.40	1.30	0.80	0.80	0

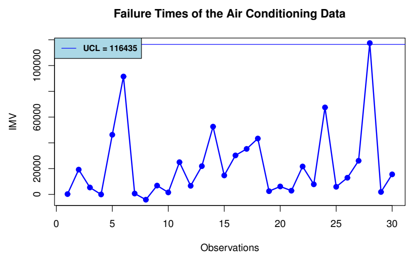

(a) IMV_t Chart at $\alpha = 0.0027$

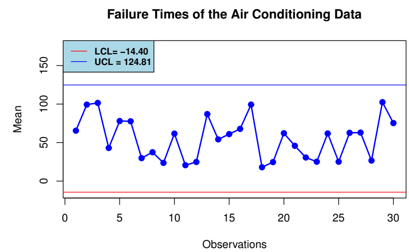

(b) Traditional chart at $\alpha = 0.0027$

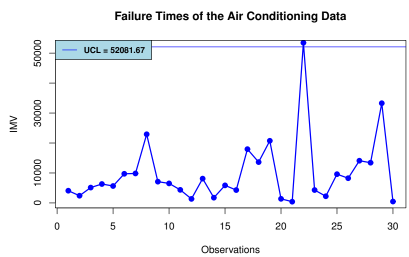

(c) IMV_t Chart at $\alpha = 0.0047$

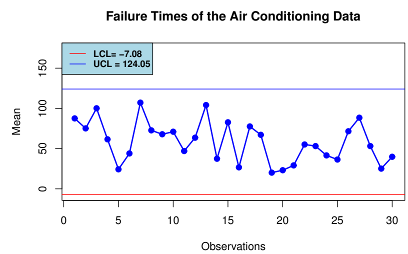

(d) Traditional Chart at $\alpha = 0.0047$

Figure 2 – IMV_t and Traditional Gamma Charts for the Failure Times of the Air Conditioning Data.

3.2.1. *Real Data Application for the Gamma IMV_t Chart*

A real life data set is taken from Gupta and Kundu (2003) which is about the failure times of the air conditioning system. The traditional gamma mean chart is also implemented to show the superiority of the proposed chart. Control limits for the traditional gamma mean charts are constructed by using Equations (18) and (19). In particular, control charts are constructed using $\alpha = 0.0027$ and $\alpha = 0.0047$, respectively. The graphical depiction of the charts is given in Figure 2. It is noticed from frame (a) of Figure 2 for α=0.0027 that the traditional gamma mean control chart does not indicate any out-of-control signal but IMV_t chart depicted in frame (b) of Figure 2 does indicate out-of-control alarm at the fourth sample. Similarly, for α=0.0047 in frame (d) of Figure 2, the traditional gamma mean control chart gives no out-of-control signal while IMV_t control chart, (frame (c) of Figure 2) gives out-of-control signals at the twenty-second observation for the failure times of the air conditioning system data. Thus, gamma IMV_t chart detects the out-of-control signals more efficiently than the traditional control charts.

3.3. *Exponential Distribution*

Exponential distribution is a continuous probability distribution commonly used as the benchmark model in reliability analysis. This distribution has a single parameter which can be estimated by the method of maximum likelihood estimation (MLE). The MDI equation to construct the information based exponential control chart is given as

$$2nD_{KL_t}(f_t^* : f_0^* | \theta_0, r_{1t}) = 2n\left[\frac{r_{1t}}{\mu_{10}} - \log\frac{r_{1t}}{\mu_{10}} - 1\right]. \tag{23}$$

Monte Carlo simulations have been used to find the upper percentile assuming $\theta_0 = 1$, $\alpha = 0.0027$ and $\alpha = 0.0047$ for different n as listed in Table 10 based on 100000 replications.

TABLE 10

Upper Percentiles of the IM_t Chart for Exponential Distribution at $\alpha = 0.0027$ and $\alpha = 0.0047$.

n	α=0.0047	α=0.0027
3	8.35	9.39
4	8.28	9.33
5	8.26	9.30
6	8.18	9.10
7	8.15	9.00
8	8.10	8.96
9	8.07	8.95
10	8.05	8.93
11	8.02	8.90
12	8.00	8.88
13	7.98	8.85
14	7.96	8.83
15	7.93	8.80

3.3.1. *Average Run Length for the Exponential IMV_t Chart*

The results for ARL_0 and $SDRL_0$ are tabulated in Table 11 based on 100000 Monte Carlo simulation runs. It can be observed from Table 11 that, for $\alpha = 0.0027$ and $\alpha = 0.0047$, ARL_0 varies with different sample sizes and at sample $n = 5$, we achieved the require in-control ARL_0. Moreover, Table 12 introduces different downward and upward shifts to evaluate the performance of exponential IMV_t control chart. The in-and out-of-control ARL values for the exponential IMV_t control chart assuming $n = 5$ are discussed for different downward and upward shift sizes. It is clear from Table 12 that the downward shifts are detected more quickly as compared to the upward shifts.

TABLE 11
ARL and SDRL for information mean chart for exponential distribution.

α	n	3	4	5	6	7	8	9	10	11	12	13	14	15
0.0027	ARL	346.87	349.38	372.80	335.85	321.10	328.60	326.55	315.30	316.50	325.40	330.28	320.38	308.00
	SDRL	348.44	352.30	372.80	330.28	320.97	340.10	321.20	307.90	315.80	325.20	333.34	318.85	303.00
0.0047	ARL	201.90	207.72	216.18	208.70	205.14	204.63	205.70	206.50	199.00	199.25	203.80	198.00	193.65
	SDRL	189.94	208.60	218.600	210.68	204.95	203.40	203.94	204.44	199.40	193.26	202.80	201.00	197.24

TABLE 12
ARL and SDRL for the Information based on Exponential Distribution.

α	δ	0.5	0.6	0.7	0.8	0.9	1.0	1.1	1.2	1.3	1.4	1.5	1.6	1.7	1.8	1.9	2.0
0.0047	ARL	0.15	2.45	6.10	20.90	96.05	216.18	137.70	69.40	37.75	22.45	13.80	9.30	6.45	4.60	3.65	2.90
	SDRL	0.80	1.90	5.55	20.25	96.30	218.60	139.60	68.10	37.65	21.85	13.15	8.80	5.85	4.15	3.05	2.30
0.0027	ARL	1.50	2.75	7.53	28.20	145.65	372.80	221.40	112.30	60.70	34.0	21.10	13.75	9.25	6.70	4.90	3.75
	SDRL	0.90	2.15	6.75	27.60	144.80	372.80	221.80	113.15	59.60	32.60	20.60	13.10	8.75	5.95	4.34	3.20

3.3.2. *Real Data Application of the IMV_t Chart for Exponential Distribution*

Using the data on the strength of 1.5cm glass fibers measured at the National Physical Laboratory, England (Shanker *et al.*, 2015), we compare IMV_t chart with the traditional exponential control chart assuming $\alpha = 0.0027$ and $\alpha = 0.0047$:

$$\mathrm{UCL} = F^{-1}\left(1 - \frac{\alpha}{2}\right); \tag{24}$$

$$\mathrm{LCL} = F^{-1}(1 - \alpha). \tag{25}$$

We used Eq. (19) to construct IMV_t chart and for the traditional control chart, the limits are given in Equations (24) and (25). It is clear from Figure 3 that the control limits of the traditional control charts are wider than the IMV_t charts for both α=0.0027 and for

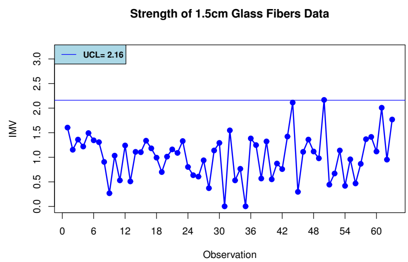

(a) IMV_t Chart at $\alpha = 0.0027$

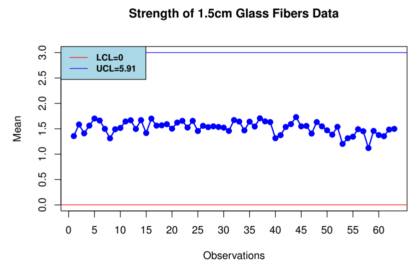

(b) Traditional chart at $\alpha = 0.0027$

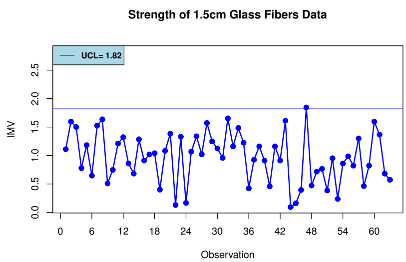

(c) IMV_t Chart at $\alpha = 0.0047$

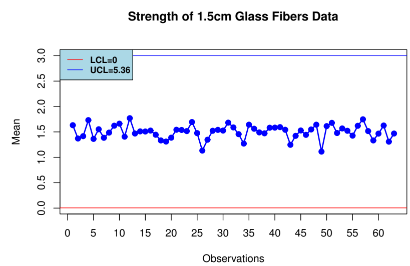

(d) Traditional Chart at $\alpha = 0.0047$

Figure 3 – IMV_t and Traditional Exponential Charts for Strength of 1.5cm Glass Fibers Data.

α=0.0047. Moreover, it is noticed from frame (a) of Figure 3 for α= 0.0027 that IMV_t control chart first out-of-control alarm at the thirteenth observation using UCL while there is no out-of-control signal by the traditional chart (frame (b) of Figure 3). However, the second point sample is out-of-control by the LCL(=0.19). Next, for α=0.0047, IMV_t chart (frame (c) of Figure 3) signals out-of-control at the sixth observation with UCL and fourth by the LCL(=0.22) while there is no out-of-control signal by the traditional chart (frame (d) of Figure 3). Thus, it can be said that the proposed information mean IMV_t chart is effective in detecting out-of-control signals than the traditional chart.

3.4. IMV_t Chart for Lognormal Distribution

Lognormal distribution is one of the commonly used distributions in applied statistics (Huang *et al.*, 2016). We use the MDI Eq. (26) to construct a lognormal joint mean and variance control chart by setting $\mu_0 = 0$, $\sigma_0^2 = 0.5$ for the in-control process with $\alpha = 0.0027$ and $\alpha = 0.0047$. The lower and upper percentiles of the joint lognormal control chart are given in Table 13 based on 100000 Monte Carlo simulations. It can be noticed from Table 13 that for both α, the LCL and UCL become wider as the sample size increase

$$2nD_{KL_t}(f_t^* : f_0^* | \mu_{10}, \mu_{20}, r_{1t}, r_{2t}) = n\left[\frac{(r_{1t} - \mu_{10})^2}{(\mu_{20} - \mu_{10})} + \left[\frac{r_{2t} - r_{1t}^2}{\mu_{20} - \mu_{10}^2} - \log\left(\frac{r_{2t} - r_{1t}^2}{\mu_{20} - \mu_{10}^2}\right) - 1\right]\right]. \tag{26}$$

TABLE 13
Lower and Upper Percentiles of IMV_t Chart for Lognormal Distribution assuming $\alpha = 0.0047$ and $\alpha = 0.0027$.

α	0.0047		0.0027	
n	LCL	UCL	LCL	UCL
3	-9.90	56.97	-10.48	63.32
4	-12.12	57.98	-12.72	70.10
5	-14.40	70.08	-15.21	76.05
6	-16.58	71.83	-16.80	88.03
7	-17.92	82.23	-18.83	92.02
8	-19.70	88.25	-20.70	94.98
9	-21.75	85.90	-22.95	105.02
10	-23.75	93.22	-23.23	108.13
11	-26.06	94.16	-26.54	116.10
12	-28.25	97.87	-28.56	117.25
13	-29.25	110.93	-29.17	122.85
14	-31.27	111.05	-32.08	134.62
15	-31.63	113.63	-32.70	134.90

3.4.1. *Average Run Length of the IMV_t Chart assuming Lognormal Distribution*

To evaluate the performance of the joint lognormal control chart, we introduce artificial shifts in the process and study its performance. It can be observed from Table 14 that as n increases the ARL_0 and $SDRL_0$ varies from sample to sample for both α=0.0027 and α=0.0047, but the require in-control ARL_0 is achieved for both α=0.0027 and α=0.0047 at sample of size $n = 5$. Table 15 refers to the ARL for $\alpha = 0.0047$ while Table 16 for $\alpha = 0.0027$ for $n = 5$ using 100000 Monte Carlo simulation replications.

TABLE 14
ARL and SDRL for information mean variance chart for lognormal distribution at α=0.0027 and α=0.0047.

α	n	3	4	5	6	7	8	9	10	11	12	13	14	15
0.0027	ARL	349.36	336.10	374.50	322.40	330.30	306.15	354.35	130.00	330.90	318.95	175.85	316.80	181.73
	SDRL	351.24	332.60	372.40	317.40	340.62	307.90	335.40	131.15	327.40	308.10	181.72	312.85	171.90
0.0047	ARL	172.25	171.68	214.30	200.90	154.56	137.78	146.50	157.40	185.48	193.25	160.05	176.83	140.17
	SDRL	152.32	163.30	216.30	202.10	157.80	135.20	153.60	163.56	177.23	188.90	154.32	178.92	125.10

It can be noticed from Table 15 and Table 16 that the chart detects efficiently upward mean and variance shifts. For fixed variance, mean is detected more quickly as the SDRL decreases with the shift size.

TABLE 15

ARL and SDRL for the IMV_t Chart for lognormal distribution with $\alpha = 0.0047$.

k	0.5		0.6		0.7		0.8		0.9		1.0	
δ	ARL	SDRL	ARL	SDRL	ARL	SDRL	ARL	SDRL	ARL	SDRL	ARL	SDRL
0.0	214.30	216.30	68.28	66.80	28.50	28.30	14.60	14.10	9.25	8.65	6.65	6.10
0.1	112.55	111.30	44.40	44.40	20.03	19.20	11.35	10.72	7.50	6.95	5.45	5.01
0.2	62.23	61.60	30.0	30.0	14.8.0	14.5.0	9.0	8.75	6.22	5.80	4.75	4.20
0.3	36.85	35.60	20.50	19.90	11.65	10.82	7.20	6.85	5.30	4.70	4.10	3.55
0.4	22.57	21.98	14.50	14.10	8.90	8.50	5.83	5.36	4.50	3.90	3.47	2.91
0.5	15.65	15.06	11.0	10.60	6.96	6.24	4.92	4.30	3.96	3.35	3.15	2.60
0.6	11.15	10.51	8.30	7.85	5.75	5.15	4.22	3.70	3.85	2.87	2.82	2.30
0.7	8.45	7.60	6.50	6.06	4.70	4.10	3.60	3.05	2.93	2.35	2.50	1.94
0.8	6.62	6.10	5.20	4.80	3.95	3.30	3.11	2.56	2.58	2.10	2.23	1.66
0.9	5.42	4.75	4.30	3.75	3.33	2.82	2.75	2.20	2.28	1.70	2.05	1.50
1.0	4.64	4.06	3.60	3.0	2.88	2.27	2.40	1.90	2.10	1.55	1.90	1.30

TABLE 16

ARL and SDRL of the IMV_t Chart for lognormal distribution at $\alpha = 0.0027$.

k	0.4		0.5		0.6		0.7		0.8		0.9		1.0	
δ	ARL	SDRL	ARL	SDRL	ARL	SDRL	ARL	SDRL	ARL	SDRL	ARL	SDRL	ARL	SDRL
0.0	360.10	360.0	374.50	372.40	81.85	81.80	26.70	26.30	11.90	11.0	6.80	6.15	4.74	4.16
0.1	327.80	320.30	175.83	175.05	50.60	50.55	18.95	18.60	9.40	9.15	5.60	5.10	3.96	3.40
0.2	110.40	108.40	88.50	88.0	33.25	33.14	13.70	13.10	7.25	6.70	4.60	4.16	3.45	2.90
0.3	48.55	48.15	49.70	48.90	22.10	21.50	10.0	9.7.0	5.80	5.25	3.80	3.25	2.97	2.40
0.4	25.70	25.05	30.90	30.24	15.75	15.50	8.0	7.95	4.70	4.25	3.30	2.75	2.60	2.10
0.5	16.14	15.40	20.75	20.30	11.50	10.80	6.16	5.80	3.90	3.40	2.90	2.30	2.30	1.70
0.6	11.70	11.40	14.35	14.0	8.60	7.95	4.90	4.20	3.30	2.90	2.45	1.90	2.10	1.45
0.7	9.45	8.90	10.90	10.50	6.60	6.40	3.90	3.40	2.80	2.20	2.20	1.60	1.90	1.30
0.8	8.20	7.65	8.25	7.70	5.10	4.60	3.35	2.85	2.45	1.90	2.0	1.35	1.70	1.05
0.9	7.50	7.10	6.80	6.15	4.10	3.60	2.80	2.30	2.20	1.50	1.75	1.15	1.50	1.0
1.0	7.0	6.50	5.35	4.90	3.30	2.70	2.34	1.80	1.90	1.30	1.60	1.10	1.20	0.90

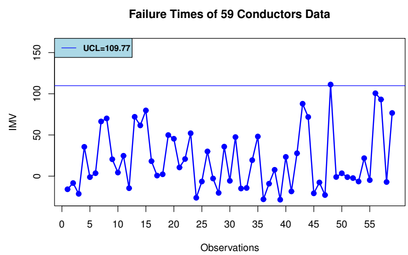

(a) IMV_t Chart at $\alpha = 0.0027$

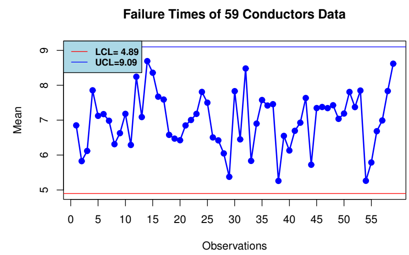

(b) Traditional chart at $\alpha = 0.0027$

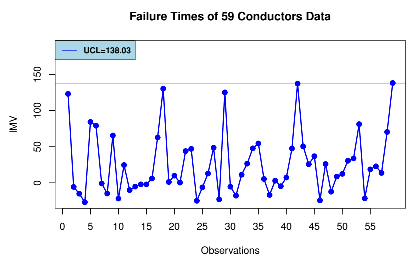

(c) IMV_t Chart at $\alpha = 0.0047$

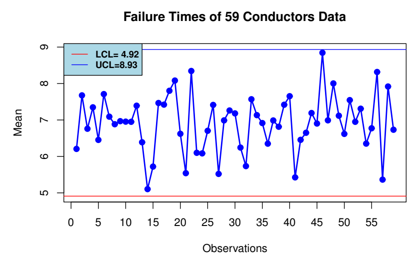

(d) Traditional Chart at $\alpha = 0.0047$

Figure 4 – IMV_t and Traditional Control Charts for Log-normal Distribution for Failure Times of 59 Conductors.

3.4.2. *Real Life Example for IMV_t Lognormal Chart*

A real life data set of failure times of 59 conductors in hours is taken from Doostparast *et al.* (2013) to present the comparison of traditional mean and IMV_t charts using $\alpha = 0.0027$ and $\alpha = 0.0047$, respectively.

The upper and lower percentiles of IMV_t are calculated by using the MDI Eq. (26) whereas the traditional mean chart control limits are computed by using the Equations (18) and (19). It can be seen from frame (a) of Figure 4 for α=0.0027, IMV_t chart signals the first out-of-control alarm at the twenty-eights sample with UCL while there is no out-of-control signal detected by the traditional chart depicted in frame (b) of Figure 4. Also, for α=0.0047, IMV_t chart signals the first out-of-control signal at the forty-ninth sample (frame (c) of Figure 4) with UCL while no out-of-control signal detected by the traditional chart (frame (d) of Figure 4). With the $LCL(= 27.47)$, the fourth point is out-of-control by the IMV chart. We conclude that the lognormal information mean-variance chart IMV_t detects out-of-control signals more rapidly as compared to the traditional chart.

3.5. IMV_t Chart for Weibull Distribution

Weibull distribution is a two-parameter positively skewed continuous probability distribution which is commonly used in statistics and reliability. We construct the information based mean-variance chart using the MDI equation for the Weibull distribution. We set in-control parameters $k_0 = 1$ and $\theta_0 = 1$ and set the in-control $ARL_0 = 150$ for the Weibull distribution. Further, the unknown parameters k_t and θ_t are estimated using the likelihood method with Nelder-Mead iterative search (Delignette-Muller *et al.*, 2015; Holland and Fitz-Simons, 1982). The MDI equation is

$$2nD_{KL_t}(f_t^* : f_0^* | \mu_{10}, \mu_{20}, r_{1t}, r_{2t}) = 2n\left[\log\frac{k_t}{k_0} + \left(\frac{\theta_t}{\theta_0}\right)^{k_t}\Gamma\left(1+\frac{k_t}{k_0}\right) - 1 - \log\frac{r_{1t}}{\mu_{10}} + (k_t - k_0)r_{2t}\right] \tag{27}$$

and the percentiles are listed in Table 17 based on 100000 Monte Carlo simulation replications. It is noticed from Table 17 that as the sample size increases, the percentiles decrease.

TABLE 17
Upper and lower percentiles for Weibull distribution at α=0.0047.

n	3	4	5	6	7	8	9	10	11	12	13	14	15
LCL	2.37	0.30	-0.50	-0.70	-1.00	-3.22	-3.92	-3.95	-4.12	-6.82	-6.90	-7.90	-8.10
UCL	148.23	29.27	28.70	28.28	27.90	27.30	23.07	22.90	22.66	22.05	20.98	20.20	20.05

3.5.1. Average Run Length of the IMV_t Weibull Chart

We evaluate the performance of IMV_t control chart using the ARL by introducing shifts of different sizes. Table 18 is based on 100000 Monte Carlo simulations to assess the effect of sample size to achieve the $ARL_0 = 150$. Next, we introduce shifts in the pro-

TABLE 18
ARL and SDRL for IMV_t chart for Weibull distribution.

n	3	4	5	6	7	8	9	10	11	12	13	14	15
ARL	89.40	58.20	52.20	77.06	130.10	159.15	84.65	73.43	90.60	69.30	55.30	89.30	70.71
SDRL	76.20	57.02	49.45	69.36	94.20	78.80	72.74	72.26	61.70	52.50	51.40	88.78	78.10

cess parameters. Tables 19, 20, and 21 list the ARL_1 values assuming a fixed scale and shifted shape, fixed shape and shifted scale, and both parameters shifted simultaneously, respectively. It clear that the chart detects out-of-control signal quickly when there is a simultaneous shift in both scale and shape parameters of the Weibull distribution. Also, the SDRL decreases as the shift size increases.

TABLE 19
ARL and SDRL for shift in k and fixed θ_0.

δ	0.5	0.6	0.7	0.8	0.9	1.0	1.1	1.2	1.3	1.4	1.5	1.6	1.7	1.8	1.9	2.0
ARL	2.29	3.60	16.10	97.94	127.70	159.15	118.10	53.56	17.70	5.80	3.20	1.83	1.40	1.20	1.15	1
SDRL	1.70	3.25	14.45	89.05	84.10	78.80	81.84	49.43	17.25	4.80	3.05	1.20	0.80	0.45	0.40	0.20

TABLE 20
ARL and SDRL when shift in θ while k_0 is fixed.

δ	0.5	0.6	0.7	0.8	0.9	1.0	1.1	1.2	1.3	1.4	1.5
ARL	1.0	1.0	1.05	3.10	76.56	159.15	16.13	2.10	1.20	1.0	1.0
SDRL	0	0	0.20	2.46	64.05	78.80	15.12	1.40	0.40	0.10	0

TABLE 21
ARL and SDRL when both parameters θ and k Shifted Simultaneously.

δ	0.5	0.6	0.7	0.8	0.9	1.0	1.1	1.2	1.3	1.4	1.5
ARL	1.0	1.0	1.04	1.75	29.05	159.15	5.05	1.10	1.05	1.0	1.0
SDRL	0	0	0.10	1.10	28.90	78.80	4.10	0.40	0.20	0	0

3.6. *Real Data Application of the IMV_t Chart for the Weibull Distribution*

Real life data on the endurance of deep groove ball bearings is taken from Gupta and Kundu (2001) to show the comparison of the proposed chart with the traditional Weibull mean chart. We estimate the unknown parameters k_t and β_t by using the maximum likelihood method with Nelder-Mead iterative search (Delignette-Muller *et al.*, 2015). The control limits for the traditional Weibull mean chart is set by using the Equations (18) and (19). The resulting comparison of control charts is depicted in Figure 5. It can be observed from the figure that the control limits for Weibull IMV_t chart are wider than the traditional chart. Moreover, it can be noticed from frame (a) of Figure 5 that IMV_t control chart signals the second sample as the out-of-control with UCL and third sample by the LCL(=10506.6), whereas from frame (b) of Figure 5, it is noticed that the

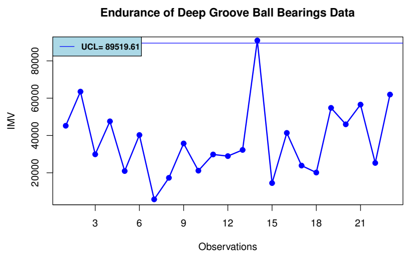

(a) IMV_t Chart

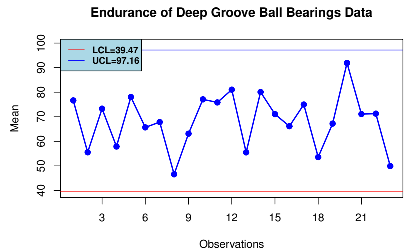

(b) Traditional chart

Figure 5 – IMV_t and Traditional Control Charts for Weibull Distribution for Ball Bearings Data assuming $\alpha = 0.0047$.

traditional chart doe snot signal. Hence, the IMV_t control chart for Weibull distribution outperforms then the traditional Weibull mean chart in detecting out-of-control signals.

3.7. *IMV_t Chart for Beta Distribution*

Beta distribution is a two-parameter continuous probability distribution and here we use it to study the performance of the information theoretic chart. The MDI equation for beta distribution is

$$2nD_{KL_t}(f_t^* : f_0^* | \mu_{10}, \mu_{20}, r_{1t}, r_{2t}) = 2n\left[-\log\frac{B(k_t \beta_t)}{B(k_0 \beta_0)} - (k_t - k_0)r_{1t} - (\beta_t - \beta_0)r_{2t}\right] \tag{28}$$

and to construct the control chart we set the in-control parameters $k_0 = 1$, $\beta_0 = 1.5$ and α=0.0047. The unknown parameters k_t and β_t are estimated by the maximum likelihood method using the Nelder-Mead iterative search (Delignette-Muller *et al.*, 2015; Holland and Fitz-Simons, 1982). We used Monte Carlo simulation to estimate unknown parameters and to find the lower and upper percentile of the beta distribution. The results are listed in Table 22 based on 100000 Monte Carlo simulation runs. It is noticed as the sample size increases, the difference between lower and upper percentile becomes small.

TABLE 22
Lower and Upper percentiles of IMV_t Chart for Beta Distribution at $\alpha = 0.0047$.

n	3	4	5	6	7	8	9	10	11	112	13	14	15
LCL	-65.21	-65.20	-42.10	-40.37	-39.15	-37.30	-33.90	-32.10	-13.67	-9.15	-6.80	-6.40	-5.75
UCL	-14.90	-13.10	-12.74	-11.95	-10.67	-10.23	-9.90	-8.84	-7.65	-6.10	-5.95	-4.60	-3.10

3.7.1. Average Run Length of the Beta IMV_t Chart

This Section discusses the efficiency of the IMV_t beta control chart. To this end, we set $\alpha = 0.0047$ and fix ARL ≈ 200. The in-control ARL_0 is achieved at sample $n = 9$ and then we introduce shifts in the process to assess the out-of-control performance. The results are listed in Tables 23, 24, and 25 based on 100000 Monte Carlo simulation replications for $n = 9$. It is seen from the tables that when there is an upward shift in the scale parameter β the proposed chart detects out-of-control signals more rapidly.

TABLE 23
ARL and SDRL of IMV_t chart for beta distribution assuming simultaneous shifts in k_0, and β_0 at $\alpha = 0.0047$.

δ	1.5	1.6	1.7	1.8	1.9	2.0	2.1	2.2	2.3	2.4	2.5
ARL	205.10	176.95	137.87	121.00	71.80	29.10	16.15	9.60	5.45	3.60	2.85
SDRL	96.40	77.20	89.90	82.43	66.55	29.20	16.85	9.30	4.80	3.10	2.30

TABLE 24

ARL for the IMV_t charts when k shifted for fixed β_0.

δ	1.5	1.6	1.7	1.8	1.9	2.0	2.1	2.2	2.3	2.4	2.5	2.6	2.7	2.8	2.9	3.0
ARL	205.10	170.70	162.00	147.55	143.56	140.30	130.51	116.50	104.15	85.80	53.55	32.00	19.70	11.20	7.90	5.30
SDRL	96.40	80.86	77.40	88.20	87.95	87.96	85.40	87.75	81.05	70.10	52.65	30.25	19.20	9.90	7.50	4.80

TABLE 25
ARL for the IMV_t charts when β varies for fixed k_0.

δ	1.5	1.6	1.7	1.8	1.9	2.0	2.1	2.2	2.3	2.4	2.5	2.6	2.7	2.8	2.9	3.0
ARL	205.10	149.25	138.60	133.10	99.10	57.65	29.55	16.65	11.15	7.25	4.90	3.95	3.30	2.80	2.20	2.00
SDRL	96.40	96.25	86.34	84.05	79.10	52.70	29.60	14.90	10.75	6.65	4.45	3.25	2.70	2.36	1.55	1.30

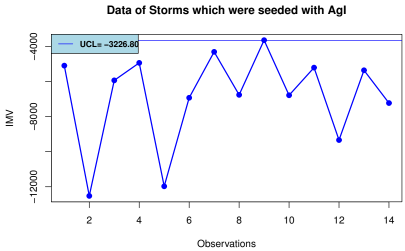

(a) IMV_t control chart

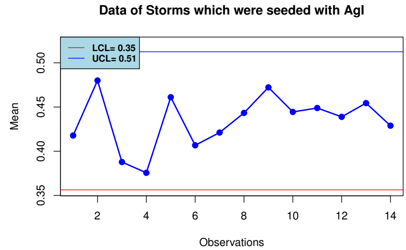

(b) Traditional chart

Figure 6 – IMV_t and Traditional Control Charts for Beta Distribution using Lear jet aircraft data at $\alpha = 0.0047$.

3.7.2. *Real Data Example of the Beta* IMV_t *Chart*

A real data set of Storms which were seeded with AgI by a Lear jet aircraft is taken from Mielke Jr (1975) and both the traditional and IMV_t control charts are constructed. The unknown parameters k_t and β_t are estimated by using the maximum likelihood method with Nelder-Mead iterative search. The IMV_t and the traditional beta charts are constructed by using Equations (18) and (19). The resulting comparison is depicted in Figure 6. It can be noticed from frame (a) of Figure 6 that the chart signals 10^{th} sample as the out-of-control with the LCL(=-13656.98) while thirteenth with the UCL. However, frame (b) of Figure 6 of the traditional chart does not signal any out-of-control observation. Thus, the beta mean-variance information chart outperforms the traditional beta mean chart in detecting an out-of-control signal.

4. Conclusion

This study assessed the performance of the univariate joint monitoring process control charts by using the information theoretic criteria based on the entropy laws and Kullback-Libeler statistic. To this end, the minimum discrimination information (MDI) equations are formulated to monitor jointly mean and variance using a single control chart. We considered different distributions, including, normal, gamma, Weibull, log-normal, exponential, and beta, and assessed the performance using different shift sizes. Based on the Monte Carlo simulations as well as real life data sets, it is noticed that the proposed charts are efficient than the traditional charts. It is worth mentioning that the likelihood ratio statistic often works better than multiple standardised statistics combinations. But still, a combination of isolated statistics, each focusing on a different aspect, is preferred because it helps post-signal screening of the problematic characteristic (parameter), which is is not possible with the overall likelihood ratio.

In this research work, we formulated univariate joint monitoring schemes using information theoretic criteria. However, in future, the work can be extended to multivariate joint process monitoring assuming different distributions. Furthermore, adaptive and self-starting memory-type charts can also be introduced.

Acknowledgements

The authors would like to thanks the anonymous referees and editor for their constructive comments to improve the quality and presentation of the work.

APPENDIX

A. MINIMUM DISCRIMINATION INFORMATION

TABLE A.1
Examples of Minimum Discrimination Information.

ME Distribution	Moments Equation	MDI Function $D_{\text{KL}}(f_t : f_0^*)$
Normal	$\mu_1 = \mu$	
$f(z\|\mu,\sigma^2) = \frac{1}{\sigma^2\sqrt{2\pi}} e^{-(z-\mu)^2/2\sigma^2}$	$\mu_2 = \sigma^2$	$\frac{(r_{1t}-\mu_{10})^2}{2\mu_{20}} + \frac{1}{2}\left[\frac{r_2 t}{\mu_{20}} - \log\frac{r_2 t}{\mu_{20}} - 1\right]$
Laplace		
$f(z\|\theta) = \frac{1}{2\theta} e^{-\frac{\|z\|}{\theta}}$	$\mu_1 = \theta$	$\left[\frac{r_1 t}{\mu_{10}} - \log\frac{r_1 t}{\mu_{10}} - 1\right]$
Exponential		
$f(z\|\theta) = \frac{1}{\theta} e^{-\frac{z}{\theta}}$	$\mu_1 = \theta$	$\left[\frac{r_1 t}{\mu_{10}} - \log\frac{r_1 t}{\mu_{10}} - 1\right]$
Gamma	$\mu_1 = k\theta$	
$f(z\|k,\theta) = \frac{z^{k-1}e^{-z/\theta}}{\theta^k\Gamma(k)}$	$\mu_2 = \log\theta + \psi(k)$	$-\log\frac{(\theta_t)^{k_t}\Gamma(k_t)}{(\theta_0)^{k_0}\Gamma(k_0)} + \frac{r_{1t}}{\mu_{10}} k_0 - k_t + (k_t - k_0) r_{2t}$
Weibull	$\mu_1 = \theta^k$	
$f(z\|k,\theta) = \frac{k}{\theta}\left(\frac{z}{k}\right)^{k-1} e^{-(z/\theta)^k}$	$\mu_2 = \log\theta + \frac{\psi(1)}{k}$	$\log\frac{k_t}{k_0} + \left(\frac{\theta_t}{\theta_0}\right)^{k_t}\Gamma\left(1+\frac{k_t}{k_0}\right) - 1 - \log\frac{r_{1t}}{\mu_{10}} + (k_t - k_0) r_{2t}$
Lognormal	$\mu_1 = \sigma$	
$f(z\|k,\theta) = \frac{1}{zk\sqrt{2\Pi}} e^{-\frac{(\log z-\theta)^2}{2k^2}}$	$\mu_2 = k^2 + \theta^2$	$\frac{(r_{1t}-\mu_{10})^2}{2(\mu_{20}-\mu 10)} + \frac{1}{2}[\frac{r_{2t}-r_{1t}^2}{\mu_{20}-\mu_{10}^2} - \log\left(\frac{r_{2t}-r_{1t}^2}{\mu_{20}-\mu_{10}^2}\right) - 1]$
Beta	$\mu_1 = \psi(k) - \psi(k+\theta)$	
$f(z : k,\theta) = \frac{z^{k-1}(1-z)^{\theta-1}}{\Gamma(k)\Gamma(\theta)}$	$\mu_2 = \psi(\theta) - \psi(k+\theta)$	$-\log\frac{B(k_t\beta_t)}{B(k_0\beta_0)} - (k_t - k_0) r_{1t} - (\beta_t - \beta_0) r_{2t}$

REFERENCES

N. AHMED, S. ALI, I. SHAH (2022). *Type-I censored data monitoring using different conditional statistics*. Quality and Reliability Engineering International, 38, no. 1, pp. 64–88.

S. ALI (2017). *Time-between-events control charts for an exponentiated class of distributions of the renewal process*. Quality and Reliability Engineering International, 33, no. 8, pp. 2625–2651.

S. ALI, S. M. RAZA, M. ASLAM, M. MOEEN BUTT (2021). *CEV-Hybrid DEWMA charts* *for censored data using Weibull distribution*. Communications in Statistics-Simulation and Computation, 50, no. 2, pp. 446–461.

L. C. ALWAN, N. EBRAHIMI, E. S. SOOFI (1998). *Information theoretic framework for process control*. European Journal of Operational Research, 111, no. 3, pp. 526–542.

M. ASLAM, O.-H. ARIF, C.-H. JUN (2017). *A control chart for gamma distribution using multiple dependent state sampling*. Industrial Engineering and Management Systems, 16, no. 1, pp. 109–117.

M. ASLAM, N. KHAN, C.-H. JUN (2018). *A hybrid exponentially weighted moving average chart for COM-Poisson distribution*. Transactions of the Institute of Measurement and Control, 40, no. 2, pp. 456–461.

J. BOONE, S. CHAKRABORTI (2012). *Two simple Shewhart-type multivariate nonparametric control charts*. Applied Stochastic Models in Business and Industry, 28, no. 2, pp. 130–140.

P. L. BROCKETT (1991). *Information-theoretic approach to actuarial science: A unification and extension of relevant theory and applications*. Transactions of the Society of Actuaries, 91, no. 452, pp. 73–135.

G. CELANO, P. CASTAGLIOLA, S. CHAKRABORTI (2016). *Joint shewhart control charts for location and scale monitoring in finite horizon processes*. Computers & Industrial Engineering, 101, pp. 427–439.

S. CHAKRABORTI, M. A. GRAHAM (2019). *Nonparametric (distribution-free) control charts: An updated overview and some results*. Quality Engineering, 31, no. 4, pp. 523–544.

Y.-C. CHANG, C.-M. CHEN (2020). *A Kullback-Leibler information control chart for linear profiles monitoring*. Quality and Reliability Engineering International, 36, no. 7, pp. 2225–2248.

Y.-C. CHANG, Y.-C. WU (2022). *A parameter-free exponential control chart based on Kullback-Leibler information for time-between-events monitoring*. Quality and Reliability Engineering International, 38, no. 2, pp. 733–756.

K. CHATTERJEE, C. KOUKOUVINOS, A. LAPPA, P. ROUPA (2023). *A joint monitoring of the process mean and variance with a generally weighted moving average maximum control chart*. Communications in Statistics-Simulation and Computation, pp. 1–21.

G. CHEN, S. W. CHENG (1998). *Max chart: Combining X-bar Chart and S Chart*. Statistica Sinica, 08, no. 1998, pp. 263–271.

G. CHEN, S. W. CHENG, H. XIE (2001). *Monitoring process mean and variability with one EWMA chart*. Journal of Quality Technology, 33, no. 2, pp. 223–233.

G. Chen, S. W. Cheng, H. Xie (2004). *A new EWMA control chart for monitoring both location and dispersion*. Quality Technology & Quantitative Management, 1, no. 2, pp. 217–231.

S. Chowdhury, A. Mukherjee, S. Chakraborti (2014). *A new distribution-free control chart for joint monitoring of unknown location and scale parameters of continuous distributions*. Quality and Reliability Engineering International, 30, no. 2, pp. 191–204.

S. Chowdhury, A. Mukherjee, S. Chakraborti (2015). *Distribution-free phase ii CUSUM control chart for joint monitoring of location and scale*. Quality and Reliability Engineering International, 31, no. 1, pp. 135–151.

N. Das (2009). *A new multivariate non-parametric control chart based on sign test*. Quality Technology & Quantitative Management, 6, no. 2, pp. 155–169.

N. Das, A. Bhattacharya (2008). *A new non-parametric control chart for controlling variability*. Quality Technology & Quantitative Management, 5, no. 4, pp. 351–361.

M. L. Delignette-Muller, C. Dutang, *et al.* (2015). *Fitdistrplus: An R package for fitting distributions*. Journal of Statistical Software, 64, no. 4, pp. 1–34.

K. Derya, H. Canan (2012). *Control charts for skewed distributions: Weibull, gamma, and lognormal*. Metodoloski Zvezki, 9, no. 2, pp. 95–106.

R. Domangue, S. C. Patch (1991). *Some omnibus exponentially weighted moving average statistical process monitoring schemes*. Technometrics, 33, no. 3, pp. 299–313.

M. Doostparast, S. Deepak, A. Zangoie (2013). *Estimation with the lognormal distribution on the basis of records*. Journal of Statistical Computation and Simulation, 83, no. 12, pp. 2339–2351.

F. F. Gan (1995). *Joint monitoring of process mean and variance using exponentially weighted moving average control charts*. Technometrics, 37, no. 4, pp. 446–453.

V. Ghadage, V. Ghute (2023). *A nonparametric control chart for joint monitoring of location and scale*. Reliability: Theory & Applications, 18, no. 1(72), pp. 553–563.

R. D. Gupta, D. Kundu (2001). *Exponentiated exponential family: an alternative to gamma and weibull distributions*. Biometrical Journal, 43, no. 1, pp. 117–130.

R. D. Gupta, D. Kundu (2003). *Closeness of gamma and generalized exponential distribution*. Communications in Statistics-Theory and Methods, 32, no. 4, pp. 705–721.

S. Hao, S. Huang, J. Yang (2016). *Design of gamma control charts based on the narrowest confidence interval*. In *2016 IEEE International Conference on Industrial Engineering and Engineering Management (IEEM)*. pp. 219–223.

D. M. HOLLAND, T. FITZ-SIMONS (1982). *Fitting statistical distributions to air quality data by the maximum likelihood method*. Atmospheric Environment (1967), 16, no. 5, pp. 1071–1076.

W.-H. HUANG, H. WANG, A. B. YEH (2016). *Control charts for the lognormal mean*. Quality and Reliability Engineering International, 32, no. 4, pp. 1407–1416.

Z. JALILIBAL, A. AMIRI, M. B. KHOO (2022). *A literature review on joint control schemes in statistical process monitoring*. Quality and Reliability Engineering International, 38, no. 6, pp. 3270–3289.

E. T. JAYNES (1957). *Information theory and statistical mechanics*. American Physical Society, 106, no. 4, pp. 620–630.

J. N. KAPUR (1989). *Maximum-entropy models in science and engineering*. John Wiley & Sons, New York.

M. B. C. KHOO, S. Y. TEH, Z. WU (2010). *Monitoring process mean and variability with one double EWMA chart*. Communications in Statistics—Theory and Methods, 39, no. 20, pp. 3678–3694.

S. KULLBACK (1959). *Statistics and information theory*. J. Wiley and Sons, New York.

C. LI, A. MUKHERJEE, Q. SU, M. XIE (2016). *Design and implementation of two CUSUM schemes for simultaneously monitoring the process mean and variance with unknown parameters*. Quality and Reliability Engineering International, 32, no. 8, pp. 2961–2975.

A. MCCRACKEN, S. CHAKRABORTI (2013). *Control charts for joint monitoring of mean and variance: an overview*. Quality Technology & Quantitative Management, 10, no. 1, pp. 17–36.

P. W. MIELKE JR (1975). *Convenient beta distribution likelihood techniques for describing and comparing meteorological data*. Journal of Applied Meteorology, 14, no. 6, pp. 985–990.

D. C. MONTGOMERY (2019). *Introduction to statistical quality control*. John Wiley & Sons, New York, 8 ed.

A. MUKHERJEE, S. CHAKRABORTI (2012). *A distribution-free control chart for the joint monitoring of location and scale*. Quality and Reliability Engineering International, 28, no. 3, pp. 335–352.

A. MUKHERJEE, A. K. MCCRACKEN, S. CHAKRABORTI (2015). *Control charts for simultaneous monitoring of parameters of a shifted exponential distribution*. Journal of Quality Technology, 47, no. 2, pp. 176–192.

M. NABEEL, S. ALI, I. SHAH (2021). *Robust proportional hazard-based monitoring schemes for reliability data*. Quality and Reliability Engineering International, 37, no. 8, pp. 3347–3361.

A. RAJAN, Y. C. KUANG, M. P.-L. OOI, S. N. DEMIDENKO, H. CARSTENS (2018). *Moment-constrained maximum entropy method for expanded uncertainty evaluation*. IEEE Access, 6, pp. 4072–4082.

S. Z. RAMADAN (2018). *Joint and control charts optimal design using genetic algorithm*. Mathematical Problems in Engineering, 2018, pp. 1–10.

S. M. M. RAZA, S. ALI, I. SHAH, M. M. BUTT (2021). *Conditional mean-and median-based cumulative sum control charts for Weibull data*. Quality and Reliability Engineering International, 37, no. 2, pp. 502–526.

S. M. M. RAZA, A. F. SIDDIQI (2017). *EWMA and DEWMA control charts for Poisson-exponential distribution: conditional median approach for censored data*. Quality and Reliability Engineering International, 33, no. 2, pp. 387–399.

E. M. SANIGA (1977). *Joint economically optimal design of $\bar{x}$ and r control charts*. Management Science, 24, no. 4, pp. 420–431.

T. SAWA (1978). *Information criteria for discriminating among alternative regression models*. Econometrica: Journal of the Econometric Society, 46, no. 6, pp. 1273–1291.

R. SHANKER, H. FESSHAYE, S. SELVARAJ (2015). *On modeling of lifetimes data using exponential and Lindley distributions.* Biometrics & Biostatistics International Journal, 2, no. 5, pp. 1–10.

J. SHORE, R. JOHNSON (1980). *Axiomatic derivation of the principle of maximum entropy and the principle of minimum cross-entropy*. IEEE Transactions on Information Theory, 26, no. 1, pp. 26–37.

E. S. SOOFI, N. EBRAHIMI, M. HABIBULLAH (1995). *Information distinguishability with application to analysis of failure data*. Journal of the American Statistical Association, 90, no. 430, pp. 657–668.

Y. TAKEMOTO, I. ARIZONO (2023). *Kullback–Leibler Information Control Chart*, John Wiley & Sons, Ltd, pp. 1–10. URL https://onlinelibrary.wiley.com/doi/abs/10.1002/9781118445112.stat08408.

C.-C. TORNG, H.-N. LIAO, P.-H. LEE, J.-C. WU (2009). *Performance evaluation of a Tukey's control chart in monitoring gamma distribution and short run processes*. Proceedings of the International MultiConference of Engineers and Computer Scientists, 2, pp. 18–20.

E. M. WHITE, R. SCHROEDER (1987). *A simultaneous control chart*. Journal of Quality Technology, 19, no. 1, pp. 1–10.

L. Xue, Q. Wang, Z. He, P. Qiu (2023). *A nonparametric EWMA control chart for monitoring mixed continuous and count data*. Quality Technology & Quantitative Management. URL https://doi.org/10.1080/16843703.2023.2246765.